Investigating the protein-protein Interaction

between

Aquaporin 4 & Calmodulin

By

Zahraa Majhool

LUNDS UNIVERSITET

Department of Biochemistry and Structural Biology

Center for Molecular Protein Science

MASTER THESIS

By due permission of the Faculty of science, Lund University, Sweden.

To be defended at the department library. Date … and time ..

2020

Supervisor: Susanna Törnroth-Horsefield

Co- Supervisor: Carl Johan Hagströmer

Examiner: Derek Logan

Abstract

Around 60 million people around the world are struggling with a traumatic brain or spinal cord injury. The swelling of the brain or spinal cord happen when the water content in the CNS increase due, infection, tumor growth or brain edema. AQP4 is a membrane water channel which mediates the water flux across the blood brain barrier (BBB) and blood spinal-cord barrier (BSCB). We believe that protein-protein interactions play crucial roles in regulating human Aquaporin's by gating or trafficking, but the mechanism of how protein-protein interaction mediate water transport across the membrane remain poorly characterized. It has been suggested that AQP4 protein could be regulated by protein calmodulin through complicated and poorly characterized mechanism. It has been suggested that protein AQP4 is regulated by trafficking mechanism, through directly binding of CaM to AQP4.

In order to demonstrate this hypothesis, AQP4 was purified from P.pastoris cells and incorporated into nanodiscs. Activated CaM will be added to the nanodisc to study the binding mode between CaM and AQP4. The purified nanodisc, used for further analysis using Cryo-EM technology. By this technique we proved that AQP4 can bind to two calmodulin protein directly.

List of abbreviations

A_{280}	Absorption at 280nm
AQP	Aquaporin
BBB	Blood Brain Barrier
CaMK	Calmodilin-Dependent Protein Kinase
CMC	Critical Micelle Concentration
CNS	Central Nervous System
Cryo-EM	Cryogenic Electron Microscopy
CV	Column Volume
DO	Dissolved Oxygen
DTT	Ditiotretol
IMAC	Immobilized Metal Affinity Chromatography
IPTG	Isopropyl β-D-1-Thiogalactopyranoside
LB	Lysogeny broth
MSP	membrane Scaffold Protein
MST	Microscale Thermophoresis
MWt	Molecular Weight
OD	Optical Density
OG	Octyl β-D-glucopyranoside
PMSF	Phenylmethansulfonyl Fluoride
POPC	Dipalmitoyl-Oleoyl-PhosphatidylCholine
PTM	Post Transitional Modification
SDS-PAGE	Sodium Dodecyl Sulfate-Polyacrylamide Gel Electrophoresis

SEC	Size Exclusion Chromatography
TEV	Tobacco Etch Virus
TRIS-HCL	2-Amino-2-(Hydroxymethyl)propane-1,3-diol Hdrochloride
YPD	Yeast extract Peptone Dextrose
Å	Angstrom

Acknowledgements

First, I would like to express my sincere appreciation to my supervisor, Professor Susanna Törnroth-Horsefield who give me this opportunity to work in here group. She always welcomed me and supported me with her knowledge, without making me feel that I'm not welcome in her office. I have to thank you for this opportunity to do this wonderful project, which also helped me in doing a lot of research and coming to so many new things.

Secondary I would like to thank my co-supervisor, PhD Carl Johan Hagströmer, he taught me the methodology in the most patient way, to carry out the research work as clearly as possible. It was a great honor to work and study under this guidance. He was never unwelcomed, with positive attitude, which made this working much easier and pleasant. A person who never made me feel stupide by doing different mistake and keep telling me " it could happen to anyone".

I would also like to thank Dr. Veronika Nešverová, she was such a helpful person in all different part of my thesis, she answered all my question without hesitation. She taught me how to prepare the nanodisc and produce the best purified nanodisc for Cryo-EM. Dr. Tamim Al Jubair, to helping me with NGC system, his door was always open to me and my questions. I would also thank Kaito Wang, who helped me with the Cryo-EM analysis and data collection.

Some special words of gratitude go to my friends who have always been a major source of support when things would get a bit discouraging: first and most Yasmin Lozansson, Fahmidul Haque and Helin Hamarashid. Thank you guys for always being there for me.

Finally, and above all, I cannot begin to express my unfailing gratitude and love to my husband, Mehdi Aljawaheri, for his continued and support and understanding during my pursuit of master's degree that made the completion of thesis possible.

Table of Contents

This thesis is dedicated to my heroes of my life,
my father and my mother. My father, my first teacher, passed away of an unexpected illness. He was 67 years old but still seek for learning more and more. He taught me that
I should always look for science. He said literacy and knowledge is a every one's weapon.
"This thesis is for you dad, as I promised you to dedicate it before you leave this world."
And my dear mother, she is still alive, and the world is still beautiful and bright. She lives miles away from me, but my heart is near together. We enjoy a wonderful friendship. She continues to support, encourage and bless me in countless ways.
"My mother thank you for all your forgiveness and kindness."

1.Introduction

1.1 Research Aim and Objectives

We aim to demonstrate the direct protein-protein interaction between the transmembrane water channel Aquaporin 4 and the multifunctional calcium-binding protein Calmodulin (CaM). All orthodox AQPs contain extended C-terminus. It has been proved that the C-terminus contain phosphorylation sites and protein binding motifs, in this case a CaM-binding motif in AQP4.

In order to have the membrane protein AQP4 in a soluble, close to native environment, form for further studding we used the Nanodisc technology. The key component for preparing assembled Nanodisc is the membrane scaffold protein (MSP).

Both AQP4 and MSP were expressed in suitable vectors and purified with, Immobilized affinity chromatography (IMAC) and size exclusion chromatography (SEC). After incorporating the full length AQP4 (AQP4-M1) into the Nanodisc, activated-CaM was added to study the binding interaction .

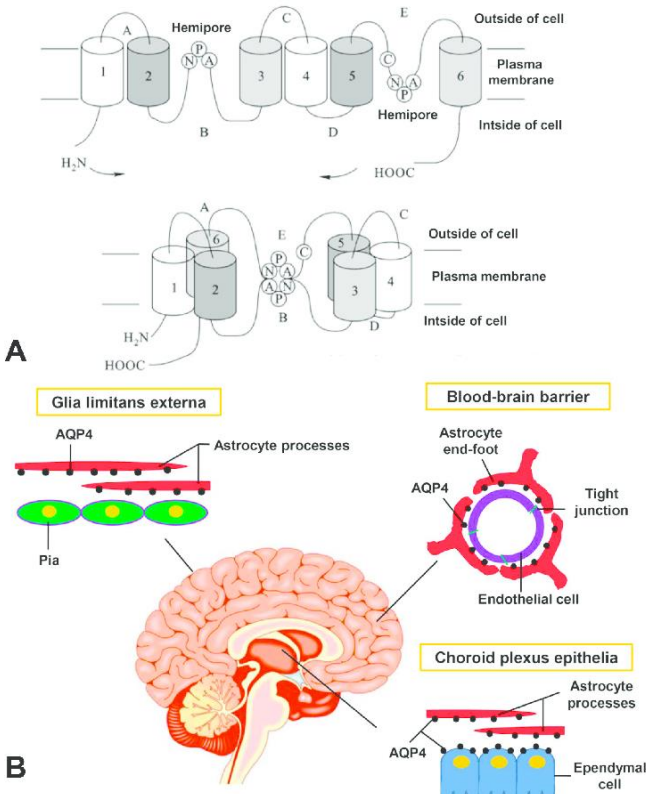

Figure 1.1 A AQP4 transmembrane helices, and highly conserved NPA-motifs which play crucial rule in water selectivity. B. illustrate the AQP4 distribution in different tissue [19].

The Cryo-EM technique was used to investigate how the AQP4 molecule interacts and functions with the protein Calmodulin. This information will be produced as a high-resolution 3D image of the protein complex, which hopefully will show AQP4 incorporated in to the Nanodisc and two CaM protein bound to the AQP4.

1.2 AQPs

For quite a long time ago we believed that the only way that the water molecule can make its their way across the cell membrane, is by diffusion through the membrane. The idea was not completely correct, because the polarity of the water molecule limits their diffusing across the hydrophobic cell membrane [1]. In 1988 Peter Agre and his coworker serendipitously isolated an unknown protein from rhesus blood group antigen (RhD), they called it CHIP28, because it is made of 28 amino acids. In 1992 they suggested that CHIP28 is a functional unit of membrane water channel, which lead to discovery of the first water transporter known as AQP1 [2].

13 different human AQPs have been discovered until now and depending on which kind of the molecule are transported through the AQPs, they are divided into three families:

- The Orthodox AQPs: permeable to water only (AQP0,1 ,2 ,4 ,5,6 and 8)
- Aquaglyceroporins: also permeable to small uncharged molecules such as, glycerol and urea (AQP3, 7, 9 and 10)
- Super-aquaporins (Subcellular-AQP): with permeability still uncertain (AQP 11 and 12) [3].

The inner pore diameter of the AQPs defines if the AQP is the water selective or can even transport other molecules. The pore diameter of the Orthodox AQPs is 2.8 Å, while the pore size of the Aquaglyceroporins can be up to 3.4 Å [4]. It has been suggested that the central pore of the AQPs can mediate gas transport such as CO_2 [5].

1.2.1 AQPs structure

All AQPs have a similar basic structure, they are a Homotetramer consisting of four identical monomers. Each monomer consist of six transmembrane helices with cytoplasmically oriented amnio and carboxy termini, each monomer act as individual water transporter (Figure 1.2.1] [6]. The AQPs facilitate water transport across the membrane by the rate of 3 Billion water molecule per second [7].In addition to the six transmembrane helices, there are two half-membrane spanning helices in the opposite sides of the transmembrane, constricting the water conductivity pore, where two NPA-motif are localized [6]. The highly conserved NPA-motif (Asparagine-Proline-Alanine) are the most important domain in AQPs that play crucial rules in water selectivity, however the function of the NPA-motif remains poorly understood. NPA-motif

consist of two copies of Asparagine-Proline-Alanine, located at the end of two short alpha-helices which is formed by loop B and E [8].

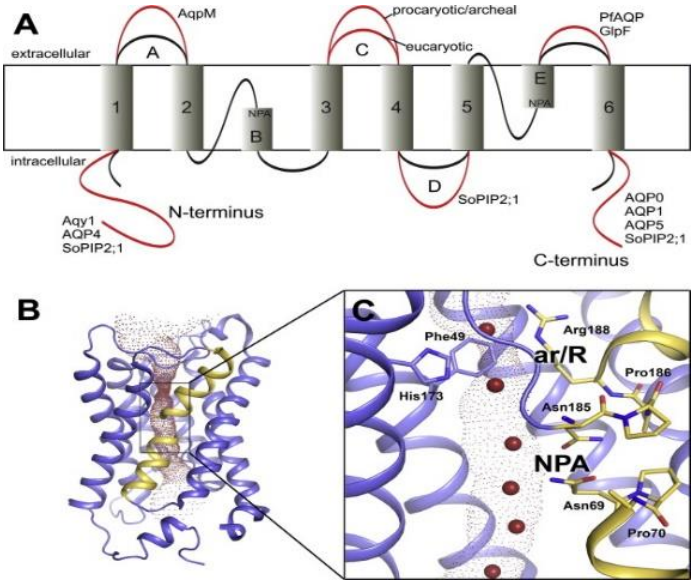

Figure 1.2.1. structural elucidation of AQPs. (A) representation the topology map, for aquaporin folding. (B) showing the overall structure of AQPs, with sex transmembrane- helices and two half-helices which enter the loop B and E presented in blue and yellow colors respectively. (C) the NPA-motif and ar/R motif, the water molecule shown in red color [12].

Additional to the NPA-motif there is a highly conserved Aromatic/Arginine, which is located near the extracellular end and act as constriction region. This ar/R prevent the passage of larger molecules and together with the NPA-region also protons [9]. This region is slightly wider in Aquaglyceroporins, to allow the transportation of the larger molecule such as glycerol [10].

1.2.2 AQPs regulation

Improper increase of the water content of the cell leads to a serious diseases, such as infection or tumor growth, for that the AQPs need to be regulated in response to cellular or environmental signals [11]. The AQPs can be regulated post-transcriptionally by so called Gating mechanisms, in which the aquaporins undergoes a conformational change, that leads to opening and closing of the channel, by which the water flux can be controlled. Trafficking is another regulatory mechanism for the aquaporins regulation, where the water channel will be translocated from storage vesicles into the surface of the plasma membrane (Figure 1.2.2) [12]. By that the density of the water channels in the plasma membrane will be altered through this regulation mechanism [13].

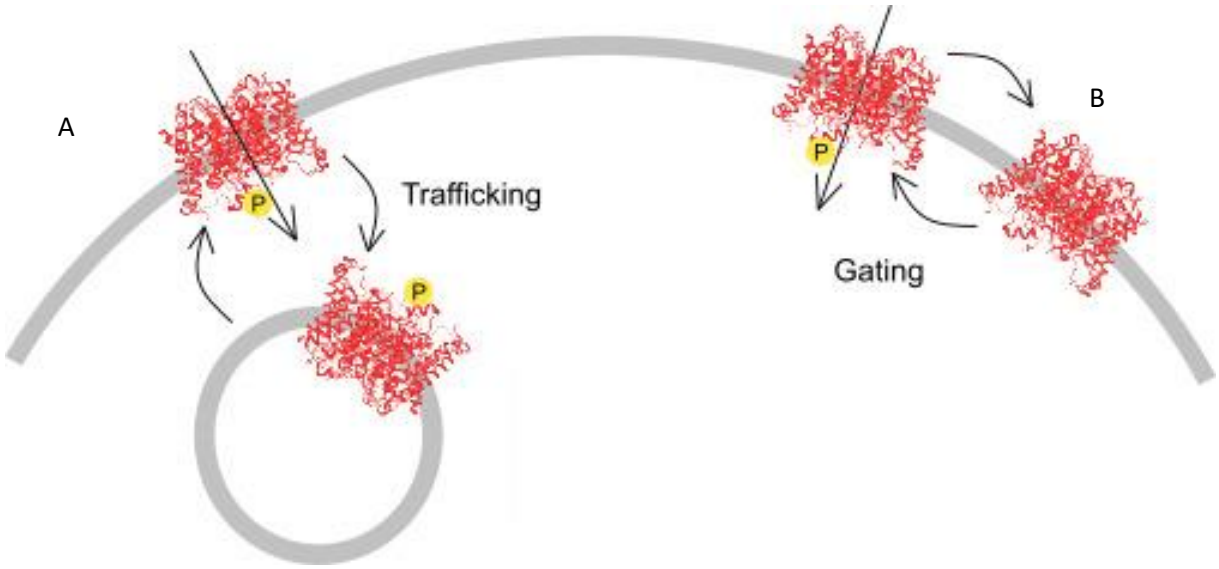

Figure 1.2.2 Illustrate the AQP regulation in the cell. A. trafficking mechanism, while the AQP translocating from the storage vesicles into the plasma membrane. B. Gating mechanism whereby AQP water flux could be controlled by the opening or closing [12].

I. Regulation of AQPs by Gating

The plant aquaporin (spinach) SoPIP2;1can be regulated by a gating mechanism, here the gating happens when the His193 at the loop D becomes protonated [14]. The protonation of the loop D, which undergoes a conformational change, leading to the formation of a salt bridge with the Asp28 residue of the N-terminus, which forms a cap for the water channel which inhibits water transportation through the membrane [15]. The pore will be opened again when the Ser115 in the loop B becomes phosphorylated, the phosphorylation leads to breakage of the interaction between loop D and N-terminus and allows transportation of the water molecules [16].

The AQP0 is another human aquaporins that has been suggested to be regulated by a gating mechanism. This aquaporin is the most abundant aquaporin in the eye lens, where it maintain lens transparency and facilitates microcirculation [17].

II. Regulation of AQPs by Trafficking

Another way to control the amount of the water that can across through the membrane, is by controlling the aquaporins density in the cell membrane, this could be trigger by phosphorylation and interactions with regulatory proteins. AQPs trafficking could involve, synthesis of AQP and constitutive targeting to the plasma membrane, or by storing the AQPs in small vesicles and use it upon special trigger [18]. When the water content of the cell increases, the aquaporin will be immerged into the cytoplasm and stored in small vesicles. On the other hand, when the water content decreases, the AQPs will be directly targeted into the plasma membrane [19]. The trafficking of the AQPs between plasma membrane and storage vesicles is a neat mechanism upon a specific trigger. The most common triggers in this mechanism are hormones such as, vasopressin, adrenalin and histamine or other small ligands such as acetylcholine and glutamate [20]. The regularity proteins are then effected by triggers, lead to activation of regulatory proteins, which in turn initiate the shuttling of AQPs into the plasma membrane [21]. The C-terminus of AQPs contain phosphorylation and protein binding sites, it has been suggested that the phosphorylation of the C-terminus leads to abrogating, inducing or changing the interaction with regulatory proteins [13].

1.3. AQP 4

AQP4 is a water selective channel, this AQP received most attention because it is highly expressed in the brain and central nervous system (CNS). AQP4 plays an important role in fluid exchange in the brain, which make it an interesting target in the case of brain edema [22]. Regulation of AQP4 is involved in various neurological disorders such as, Alzheimer, Amyotrophic lateral sclerosis, Parkinson's disease, Multiple sclerosis, Neuromyelitis Optica, Epilepsy, Traumatic brain injury and stroke [20]. It has been suggested, that the inhibition of AQP4 can reduce brain edema [23].

AQP4 share the same structural properties, as all other AQPs. This AQP has ability to aggregate in order to form supramolecular, called orthogonal array of particle (OAP) [24]. There are two isoforms of human AQP4, AQP4-M1 and AQP4-M23. The difference between these two isoforms is, that the AQP4-M1 is longer than AQP4-M23 by 22 amino acids on the N-terminal side [25]. It has been suggested, that only AQP4-M23 can form orthogonal array on its own (Figure 1.3), but AQP4-M1needs to be merged with M23 to form a small OAP [26].

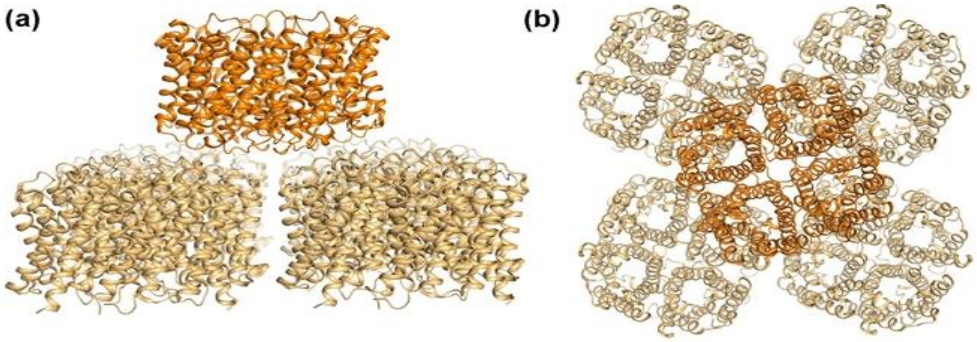

Figure 1.3. structure of AQP4 array formation. (a) illustrate a parallel view of AQP4-M23, (b) perpendicular view [25].

AQP4 could be regulated in a phosphorylation- dependent manner. The phosphorylation of Ser111 in cytoplasmic loop B leads to activation of AQP4, while the phosphorylation of Ser 180 lead to inhibition of AQP4 [27]. There are many factors that have been reported to alter AQP4 density and subcellular localization such as: vasopressin, histamine and astrocytic glutamate [26]

On the other hand, it has been proposed that AQP4 can be regulated by trafficking mechanism including protein-protein interaction. In this mechanism, the present of transient receptor potential vanilloid (TRPV4) is essential for the regulation of AQP4 [28]. This channel is, a Ca^{2+}-permeable nonselective cation channel, which plays a crucial role in mechanosensation or osmosensation in several tissues [29]. The Ca^{2+} is necessary for activation of the calmodulin protein. This mechanism includes the direct interaction between

Ca^{2+}/dependent protein calmodulin and the C-terminus of AQP4, causing a specific conformational change in the C-terminus of AQP4, leading to surface localization of the AQP4 which had been stored in small vesicles.

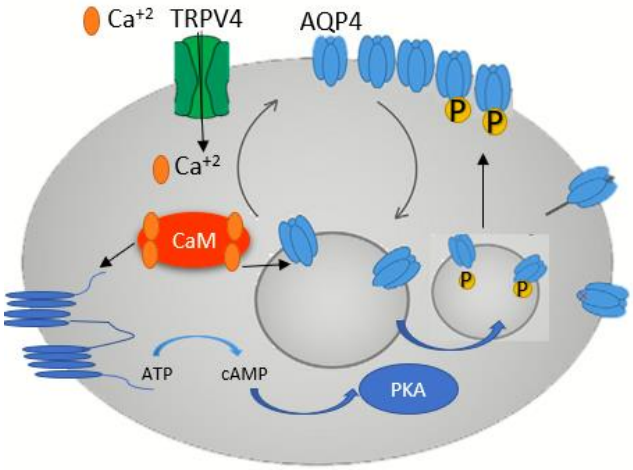

Figure 5. illustration of trafficking mechanism. The AQP4 which had been stored in vesicles, could be shuttled between vesicles and plasma membrane. This shuttling will be triggered by activation of CaM and direct binding of CaM to the AQP4. This protein-protein interaction leads to conformational change and surface localization of AQP4

1.4. Calmodulin

Calcium is an ubiquitous universal intracellular secondary messenger, which acts as a mediator in protein stimulation, coupled with example regulation of plant growth [30], development and respond to environmental stress . There are several Ca^{+2} sensors, that have ability to detect this stimulus, such as protein calmodulin (CaM), calcium dependent protein kinase (CDPK)and calcineurin B-like protein (CBL) [31].

CaM by itself has no catalytic activity, but upon binding of Ca^{+2}, it may be activated and act as secondary messenger to activate numerous downstream target proteins [32]. Calmodulin is a small, soluble, thermostable protein which has acidic properties and can be found in animals, plants, fungi and protozoa but absent in prokaryotic cells. Calmodulin is highly distributed in all body tissues and one of the most abundant proteins in the brain, where its concentration differs from 1-10 [33]. Structurally calmodulin is made of 148 amnio acids with two highly conserved symmetrical globular domains (N-domain and C-domain), each contain a pair of EF hand (a helix-loop-helix found in large family of calcium binding proteins) motifs linked to each other by a flexible region (Figure1.4) [34]. Each calmodulin molecule has ability to bind to four calcium ion molecules, two in each domain. When the CaM binds to the Ca^{2+} it undergoes a conformational change leading to exposure of the hydrophobic region of CaM which allows it to bind to the other proteins [35].

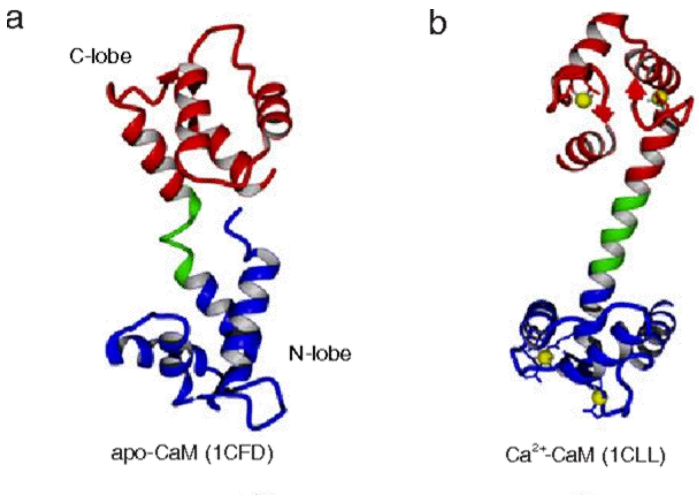

Figure 1.4. representation of the protein calmodulin, a is the protein calmodulin, which is not active, known as apo-CaM. B is the CaM-Ca^{+2} complex with new conformation in response to binding of a calcium ion. The N-domain and C-domain illustrated by blue and red respectively [34].

2.Methodology

2.1. Protein expression and purification

2.1.1. Protein overexpression

Protein expression is a method which is usually used to overexpress a specific protein in a host cell. The gene of interest which had been cloned into a suitable vector was transformed into the host cell, this host cell could be eukaryotic or prokaryotic. Depending on what features does the protein of interest has and which post-transitional modification (PTM) are important, we can choose the host cell. Once the gene of interest has been transformed into the host cell and the cell density reach the desired level, the expression will be induced using a specific reagent, varied depending on the vector type. The induction triggers a promotor in the vector, that allows overexpression of the desired protein. For the MSP protein, *E. coli* was selected as a suitable host cell. For protein expression in *E. coli*, a single colony containing the gene of the protein, was inoculated in LB media and grown in a shaking flask in 37^0 C. When the OD_{600} reach the desired density, the culture would be induced, when the cell density reaches the desired density, using IPTG as inducing reagent. This IPTG activates the T7 promotor, which leads to protein overexpression. The induction can take up to 4 hours. The cells were harvested using centrifugation and the pellet was recovered for further analysis.

Pichia- pastoris was used as host cell to grow AQP4. The advantage of this cell comes from that these cells are methylotrophic yeast, that can use only methanol as source of energy for cell growth, methanol solution has ability to kill most other micro-organism. Another advantage of *Pichia- pastoris* is a highly efficient, cost effective expression and high yield system.

The *Pichia* cell containing the gene of the protein of interest is grown in a media supplemented with glycerol, production of the protein was performed in large scale using fermenter. During the fermentation process it is important to monitor the following parameters: PH 5-6 (important for optimal growth), temperature 30.0°C (above 32 ° C is harmful for protein expression), dissolved oxygen or DO >20% (*Pichia* needs oxygen to metabolize glycerol and methanol). Once all glycerol which had been in the media growth batch was

consumed by the cells, a glycerol feed was initiated to increase cell biomass under controlled condition. The DO spikes could be monitored to make sure the glycerol is limited to start inducing the cells with methanol. It is necessary to make sure that all glycerol had been consumed before starting with methanol feeding, to fully induce AOX1 promoter (alcohol oxidase 1, this promotor heavily induced in present of methanol) on methanol. After inducing with methanol, the cells were harvested by centrifugation and the pellet was recovered for further analysis.

2.1.2 Membrane solubilization and purification

The frozen pellet contains thousand different proteins and in order to be able to study the protein of interest *in vitro* we need to extract and purify it from the cell. At the first step the bead- beater is used to prepare the cell lysate, lysate contains debris and membrane which contain the protein of interest. Different centrifugation steps was run in order to isolate, wash and homogenize the membrane. Since the membrane proteins are made of the hydrophobic and hydrophilic parts, a suitable detergent was used to extract the proteins and keep them stable and soluble in the solution. The concentration of the detergent should be above the critical micellar concentration (CMC) to allow the micelles to start forming and to the protein to be solubilized out of the membrane. For further purification, the protein of interest was tagged by 6 Histidine residues and purified using affinity chromatography in a nickel column.

2.1.3 IMAC

Immobilized metal affinity chromatography (IMAC) is a chromatographic technique in which the metal ion will be immobilized (in our case Ni^{+2})on a solid resin through a linker such as nitrilotriacetic acid and iminodiacetic acid. The most common ion for His-tag purification of a recombinant protein is Ni^{+2} , Co^{+2} and Zn^{+2}. The His-tag has a high affinity towards metal ions, which leads to strongly binding of the protein to the column. The protein which has been tagged with poly-Histidine tag will flow through the resin and be trapped and retained by this metal supported stationary phase, while other proteins which does not contain any tag will just pass through the column. The tagged protein will be eluted from the column by changing the pH of the mobile phase, which will effect the ionic strength of the mobile phase. Another way to elute the sample from the column is to use high concentration of imidazole, imidazole has ability to compete with the His-tag for binding to the metal ions in the stationary phase and thus the protein will be eluted from the column.

2.1.4 SEC

Molecular exclusion chromatography also called size exclusion chromatography is a chromatography technique, which separates molecules depending on their size. The separation will be achieved by the fact that the larger molecules pass through most quickly. In an ideal case there will not be any interaction between the stationary phase and the solute. Rather the liquid mobile phase passes through a porous gel. The smaller molecules penetrate the pores in the stationary phase but the larger molecules stream past without entering the pores. This technique is widely used in biochemistry to purify macromolecules such as proteins. This technique uses not only as a purification step, but also as check for sample quality and homogeneity, protein aggregation could be also detected by this technique.

2.1.5 SDS-PAGE

One simple and efficient technique in protein characterization is sodium dodecyl sulphate polyacrylamide gel electrophoresis (SDS-PAGE). In general, this method separates the proteins according to their size. The application of the electric filed across the polyacrylamide gel force the proteins, which have been treated with SDS, to migrate through the gel toward the anode. The treatment of the protein with the SDS confers a constant negative charge to the protein, unfold the protein structure to be rod shape. As a result, the SDS-treated proteins migrate through the gel according to their size only, the larger molecule move slower through the gel because of the size of the pores of the gel. The protein visualization may be done by staining the gel in Coomassie Brilliant Blue or silver.

2.2. Protein structure & binding

2.2.1 Nanodisc assembly

In order to have the protein in an environment quite close to native like membrane environment, we used nanodiscs. A nanodisc is a synthetic small disk that provide a platform for membrane protein isolation, purification, structural elucidation and functional characterization, avoiding usage of detergent or liposome [36]. Another benefit of the nanodisc is that the nanodisc is stable and soluble in aqueous solution and could preserve a general stable form of the phospholipid stoichiometry. The desired protein may be incorporated into the nanodisc. The nanodisc made up of two layer of lipid bilayer and encapsulated by two copies of a membrane scaffold protein call MSP (Figure 7) [37]. The detergent that has been covering the membrane protein, this time will be replaced by the lipid bilayer. There are three different synthesized lipids that can be used, dipalmitoyl-oleoyl-phosphatidylcholine (DPPC), dipalmitoyl-oleoyl-phosphatidylcholine (POPC) and dimyristoyl-glycero-phosphocholine (DMPC), in our case we used POPC [38].

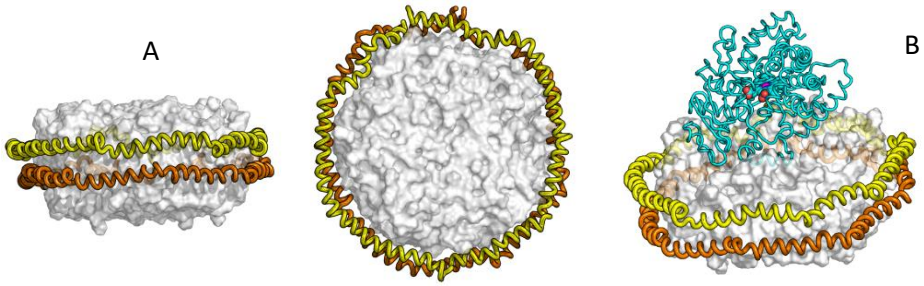

Figure . (A) side and topp view of phospholipid bilayer surrounded by, two copies of MSP. (B) membrane protein incorporated into the nanodisc shown by blue color.

(MSP) is a derivative of apolipoprotein A-1, which consist of two copies of amphipathic α-helices. The MSP construct contains an N-terminal His-tag and TEV protease cleavage site, to remove the tag after purification steps. This protein could be expressed in pET-family of vectors [39]. There are many types of MSPs which vary by length and presence of tag. There are two factors to keep in mind when choosing the MSP, the first factor is that the size of the MSP should be enough for desired protein to be reconstituted into the nanodisc, the second factor is the tag on the MSP should be efficient for the desired purifications [40].

The nanodisc assembly will start after purification and isolation of the membrane protein (MP) by detergent and purification of the MSP protein. This requires mixing of the MSP and MP in

the presence of the bio beads (the bio beads will consume the detergent from the MP) in presence of lipids. The ratio of lipid:MP:MSP is an important parameter in the nanodisc assembly. An excess of the lipid in the solution leads to non-discoidal structures formation or forming an empty nonodisc, by competing with MP for sitting in the nanodisc. Each nanodisc requires two MSP as belt to be form that is why we need at least double amount of the MSP comparing to the MP. The interaction of the MSP with the hydrophobic tail of the lipids leads to shielding the lipids from solvent, nanodisc assembly occurs when the detergent is slowly removed from the solution mixture. The incorporation of the MP into the nanodisc could be carried out during self-assembling process [40].

2.2.1. Cryo-EM

The structure of a protein is crucial to determine the function of the protein, by understanding the structure of protein and clarifying its function, it could be easier to predict the binding of other proteins and design a drug for that specific protein. Protein structures are very complex and only very recently, discovered a beneficial technique to determine the structure of complete protein down to its atomic level. One of this powerful and recently discovered technique is Cryo-Electron Microscopy (Cryo-EM) [41]. These technique which has been invented by Jacques Dubochet, Joachim Frank, and Richard Henderson, received the Nobel Prize in 2017. In this technique, the specimen is rapidly cooled down to the cryogenic temperature, leading to formation amorphous frozen solid, thus avoiding damaged caused by water crystallising. This procedure is followed by taking a series of two-dimensional images, using a high-resolution camera, and recording thousand of images on a computer. These images are then processed by reconstruction software, to produce a 3D-image of the macromolecule structure in resolution close to 2 Å [42].

3.Materials & methods

3.1. Membrane scaffold protein

3.1.1. MSP overexpression

A small amount of the BL21 E. coli, containing MSP1E3D1 plasmid with kanamycin resistance, was heat activated and plated on an agar plate (Table 1), the plate was incubated overnight at 37 °C. A single colony was then transferred to 25 ml LB media (Table 2) containing 0.05 mg/ml kanamycin, incubated on shaker for growth overnight at 37 °C. The overnight culture was then inoculated into TB media (Table 3) containing 0.05 g/l Kanamycin, was grown on vigorous shaking (150 rpm) at 37 °C to a cell density OD600= 0.6-0.8. In order to induce the protein expression, 1mM IPTG was added to the cell culture and incubated for approximately four hours. The cells were then harvested using JLA 10.5 rotor and centrifuged at 5 krpm for 30 min at 4 °C. After removing the supernatant, the pellet was resuspended in 45 ml KPO_4 buffer (Table 4) and stored in -20 °C.

3.1.2. MSP Purification

The cells were lysed using sonication. 1% Triton x-100 and 1mM PMSF was added to the lysed cells. The sonication setting was as follows: duty cycle 50, output control 6 and sonicated 3×4 min on ice. The cell mixture was then ultra-centrifuged using Ti70 rotor at 50 krpm for 1 h at 4 °C. The supernatant was collected and filtered using 0.45 μm syringe. 2×5 ml His-trap column were equilibrated with KPO_4 buffer (Table 4) and the supernatant was loaded into the column overnight at 4 °C.

The column was washed with buffer1 (Table 5), buffer 2 (Table 6) and buffer 3 (Table 7), containing different concentrations of imidazole. The MSP was than eluted from column using buffer 4 (Table 8) with the highest concentration of imidazole. The presence of the protein was proved by SDS-PAGE and the concentration was determind using Nanodrop 2000 (Thermo scientific) by measuring the absorbance at 280 nm.

3.1.3. Removal of His-Tag from MSP

The eluted MSP was mixed with TEV protease in a ratio of 1:10 w/w TEV/MSP and 1.5 mM of DTT was added to the mixture. In order to remove the high concentration of imidazole from the mixture, the sample was dialyzed against Tris buffer (Table9) for 20 h at 4 °C under continuous stirring. The dialyzed mixture was than loaded into the His-Trap column, which had been equilibrated with 20mM imidazole (Table 10) and eluted with the same buffer. The MSP was concentrated by using Vivaspin 6 with 3kD cut off centrifugation filter at 4000 rpm. SDS-PAGE was used to confirm the removal of His-tag and the concentration was measured by Nanodrop at 280 nm.

3.2. Aquaporin 4

3.2.1. AQP4 overexpression in P.pastoris

A stock solution of the human AQP4-M1 was provided by Susanna Törnroth-Horsefield and inoculated on a YPD agar plate. The YPD plate was incubated at 30°C for 3 days, the cell appeared as a greasy layer on the top of the YPD plate. A large amount of greasy colonies was then inoculated into 100 ml of YPD media (Table 11), the media was then grown on a shaker overnight at 30°C, OD600 = 25 is require for fermentation. After autoclavation of the fermenter, Basal salt media (BSM) (Table 12) was added to the fermenter and the pH of the media was adjusted to 5 using concentrated NaOH. To the BSM media, Pichia Trace Minerals (PTM) (Table 13), 100 ml YPD culture and a few antifoams drops were added. The fermenter was set up with the following parameter overnight: Temp = 30◦C, pH = 5.0 - 5.1, DO = 25, Gas = 1, Pump A = 0, Pump B = 0, Stir = 800 – 1500. After consumption of the glycerol, as the cells grows, the DO decreases and when the glycerol in BSM medium is completely consumed by the cells the DO rises sharply, this is the initial batch phase. The second phase will start, when cells are fed by 50 % glycerol which contain 1.5 % PTM in order to grow for one day. Induction of the cell occur when the feeding was switched to the methanol containing 1.5 % PTM for two days. The cells were harvested by spinning them in a centrifuge at 6000 rpm with the rotor JLA, 8.1000, Beckman Coulter. The pellet was stored in a freezing bag and stored at -20 °C.

3.2.2. Membrane preparation

Around 100 g of the frozen cells were thawed in the breaking buffer (Table 14) for about 30 min at room temperature. The cell was then disrupted using about 200 ml of the ice-cold glass beads (0.5 mm, Biospec) and a bead beater (Bead Beater, Gln Mills), along with 1mM PMSF. The bead beater was run at 12×30 Sec with 30 Sec pause in between each run (in total 12min). the cell debris and unbroken cells was then removed from the solution by centrifugation for 30 min at 9.5 krpm using JLA 10.500 rotor at 4 °C. The supernatant was then collected and centrifuged using rotor Ti 45 for 1 h, 45 krpm at 4 °C. The pellet which supposed to contain the membrane fraction was homogenized with urea buffer (Table 15) using a potter homogenizer, after homogenization, the solution was transferred in to the Ti45 tubes and centrifuged at 45 krpm at 4◦C for 2 h. The supernatant was discarded, and the pellet was further homogenized using membrane Buffer (Table 16) containing 1mM PMSF and 2mM EDTA using a potter homogenizer. The homogenized pellet was transferred to Ti 45 tubes and centrifuge at 45 krpm at 4◦C for 1h 15min. The pellet was weighed and resuspended in membrane buffer (2ml/g membrane) and homogenized. The solution, which supposed to contain AQP4 in the membrane, was aliquoted in falcon tubes and stored in -80 °C.

3.2.3. Solubilization of AQP4 from membrane

This step was done in order to extract the protein from the membrane and have it in an aqueous solution using the detergent. The membrane was solubilized by dropwise addition of the solubilization buffer (Table 17), to a ratio of 1:1 and incubated by continuously stirring in 4°C for 2.5 h. 10mM of the Imidazole was added to the final solution. The non-solubilized protein and the membrane was then removed by ultracentrifugation for 30min at 50 krpm using Ti70 rotor.

3.2.4. AQP4 Purification

In order to purify the AQP4 from other proteins in the solution we used Ni-affinity chromatography. The supernatant, which was provided from previous step, was loaded to a 5 ml His-Trap column. The column was washed in two steps, first with buffer A (Table 18) containing 10mM imidazole, second with the same buffer but this time higher concentration of imidazole which was 75 mM. AQP4 was then eluted from column with buffer B (Table 19), the purity and presence of AQP4 was verified using SDS-PAGE. The fraction containing AQP4 was pooled, aliquoted (500 µl in each tube) and stored in -80 °C. 500 µl of the purified AQP was further purified using SEC (Superdex® 200 Increase 10/300 GL), the running buffer was

Buffer A but this time without Glycerol (for the Nanodisc preparation purpose). The fraction containing desired proteins was pooled and concentrated to up to 10 mg/ml using Vivaspin 6 (MWCO 50). The concentration was determined using nanodrop 2000 (Thermo scientific) by measuring the absorbance at 280 nm.

3.3. SDS-PAGE

The sample of interest was mixed with 3×SDS loading dye, containing Dithiothreitol (DTT). The mixture was loaded onto a NuPAGE™ 4-12 % Bis-Tris Plus protein gel (Invitrogen) along with Spectra ™ Multicolor Broad Range Protein Ladder (Thermo Scientific), which was used in order to clarify the molecular weight of the proteins. After loading the denatured protein mixture and the ladder into the gel, which had been placed in the electrophoresis cell and filled with NuPAGE MES buffer (Table 20), an optimum program was chosen to provide best resolution between proteins. After migration of sample to the end of the gel, the gel was placed in water and microwaved for 30 sec and shaken for 1 min. this step should be repeated three times and every time the gel should be washed with new water. To stain the gel, we used SimplyBlue ™ Safe Stain (Novex) and microwaved for 30 sec than put on the shaking table for at list 15 min. to destain the gel, the gel was washed again with water and left on shaking table. The proteins which had been bounded to the dye could be visualized in a gel scanner (SYNGENE PX).

3.4. Nanodisc preparation

After cleavage of His-tag from MSP protein and purification of the AQP4, the AQP4 was incorporated into the nanodisc. The nanodisc consist of MSP1E3D1 and POPC lipid (Dipalmitoyl-2-Oleoyl-PhosphatidylCholine) powder. The POPC was solubilized with sodium cholate-buffer (Table 21) to concentration of 50 mM, the mixture was vortexed for approximately 30 min until the mixture become completely transparent.

The nanodisc reaction mixture consisted of POPC:MSP:MP with molar ratio 80:2.5:1. The mixture was incubated on a rotating incubator for 1 h at 4 °C. To start the assembling 0.5

g/ml of Amberlite Xad-2 biobeads was added to the reaction mixture and the mixture incubated overnight at 4 °C. after removal of biobeads the sample was loaded on a His-Trap FF 1ml column, which was equilibrated with Tris buffer (Table 22). The empty nanodisc and excess of MSP were eluted rapidly from the column, while the nanodisc containing AQP4 was eluted with buffer with high imidazole concentration (Table 23). The fraction containing nanodisc with AQP4 was pooled and concentrated in a spin concentrator with 50 kDa cut off. Further purification with Gel filtration (superdex 200 10/300 GL) was performed with nanodisc.

3.4.1. Formation of nanodisc-AQP4- CaM complex

In order to form nanodisc-AQP4-CaM complex, the CaM protein needs to be activated by $CaCl_2$. 1,2 mg of CaM protein which was provided by Sara Linse group was diluted using Tris-buffer for nanodisc (table 22) to reach the concentration of 5 mg/ml. 1mM $CaCl_2$ was added to the CaM in order to activate the protein to the ratio of 1:4 CaM: $CaCl_2$. The molar ratio of 1:10 nanodisc: activated CaM was mixed and sent for Cryo-EM sample preparation.

3.5. Cryo-EM

This part was done by our collaborator Kaituo Wang at Copenhagen University (kaituo@sund.ku.dk).

After fully saturating the AQP4 complex with CaM, 1mM of the $CaCl_2$ was added to activate the CaM and the mixture was then incubated on ice for 1 h. Quanti-foil 2/2-µm holy carbon grids (300mesh) were glow-discharged with 5mA for 30s in Leica Coater ACE 200 in glow discharge mode. Cryo-EM grids were prepared with the Vitrobot Mark IV (FEI) operated at 100 % humidity at 4 °C. 1mM Flurinated-Fos-Choline-8 was added to the sample immediately prior to plunge freezing. For each grid, an aliquot of 3.5 µL sample was applied and incubated for 10 s inside a Vitrobot. Blotting and drain times were both set to 2s with blotting force set to 0. Frozen grids are stored in LN2 until data collection. The Cryo-EM data was collected at the Umeå Core Facility for Electron Microscopy using a Titan Krios electron microscope (FEI) operated at 300 keV with a K2 direct electron detector. A dataset of 3014 Movies were recorded under counting mode at a pixel size of 0.82 Å and a total dose of 60 $e^{-}/Å^{2}$ divided into 40 frames.

4.Results & discussion

4.1. MSP purification with Ni-affinity column

The MSP protein was overexpressed in BL21 strain, which serves as a good host for MSP overexpression, harvested by centrifugation and loaded onto the IMAC (Ni-affinity) column. The column was first washed with different concentration of imidazole in order to remove the proteins which might be non-specifically bound to the column. The MSP protein which contain His-Tag and have high affinity to bind to the Ni-column was than eluted with buffer containing 400 mM imidazole. The chromatogram (Figure 4.1.1) clearly show elution of the MSP from the column. Increasing of imidazole concentration, which has high affinity to bind to the column, lead to increasing the competition between MSP and imidazole to Nickel ions sitting on stationary phase, as result the MSP will be eluted from column.

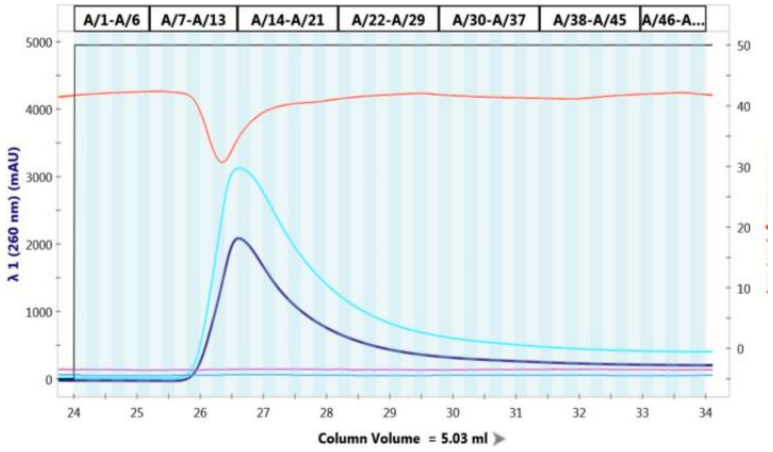

Figure 4.1.1 chromatograph represent a low scale His-Trap of MSP, the fraction A -9 to A-28 was pooled and confirmed by SDS-PAGE

The fraction containing the MSP protein was analyzed by SDS-PAGE in order to confirm the presence of desired protein. The MSP has a molecular weight of 32370 g/mol, when it contains His-Tag, from the gel (Figure 4.1.2), a high intense band on molecular close to 35 kDa is clearly represent the presence of MSP protein. The concentration of the pooled fraction measured by nanodrop to be 2.6 mg/ml.

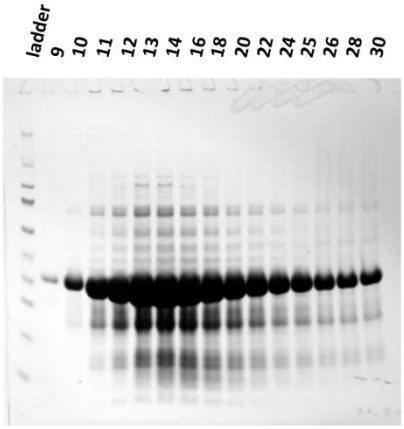

Figure 4.1.2. SDS-PAGE showing the presence of MSP protein in high intense band corresponding to the MWt of 35 kDa, MWt of MSP= 32370 Da.

4.2. Cleavage of His-tag residue from MSP

The His-tag needed to be removed for further application when we try to assemble the nanodisc. After dialyzing the protein in the presence of TEV protease, the MSP was purified and isolated from non-cleaved MSP and TEV protease using reverse IMAC. The non-cleaved MSP and TEV both contain a His-tag and therefore have high affinity to the Ni-column, while the cleaved MSP passed through the column rapidly.

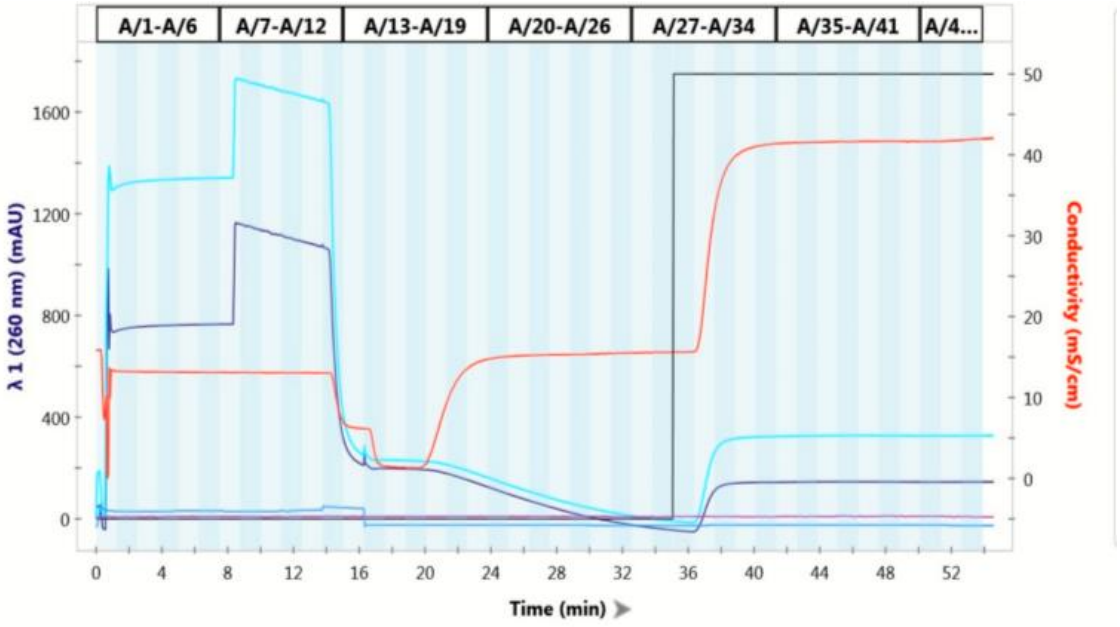

Figure 4.2.1. the chromatogram of affinity chromatography (His-trap) achieved from cleaved MSP, the fist peak(A1-A12 contain the protein, but the peak look weird) but the presence of the protein was proved using SDS-PAGE figure 4.2.1.

The first peak (Figure 4.2.1.), from A1-A12), represent the peak contained the cleaved MSP proteins. The TEV protease and the noncleaved MSP supposed to be eluted by high concentration of imidazole, but the chromatogram does not show any peak. The presence of the TEV protease and the non-cleaved MSP could not be confirmed by SDS-PAGE.

The fraction containing the cleaved MSP was analyzed by SDS-PAGE to give the following picture (Figure 4.2.1).

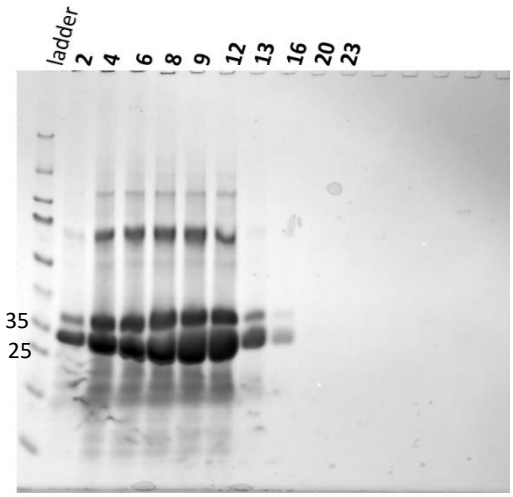

Figure 4.2.1 represent the presence of MSP, MWt of MSP protein without His-tag is 29900 g/mol. The TEv-protease which supposed to be eluted with high concentration of imidazole, was not clear and reason is unknown.

4.3. AQP4 Purification

Fermentation of P.pastoris in order to overexpress the AQP4 was efficient, 400 gr of cells, containing AQP4. After extracting the protein from cell using OG as a detergent, the sample which had been centrifuged loaded into a super loop and purified from other protein using His-trap column. The following chromatogram (Figure 4.3.1) shows elution of the AQP4 from column. The fraction (A6-A9) was used for further analysis using SDS-PAGE (Figure 4.3.1).

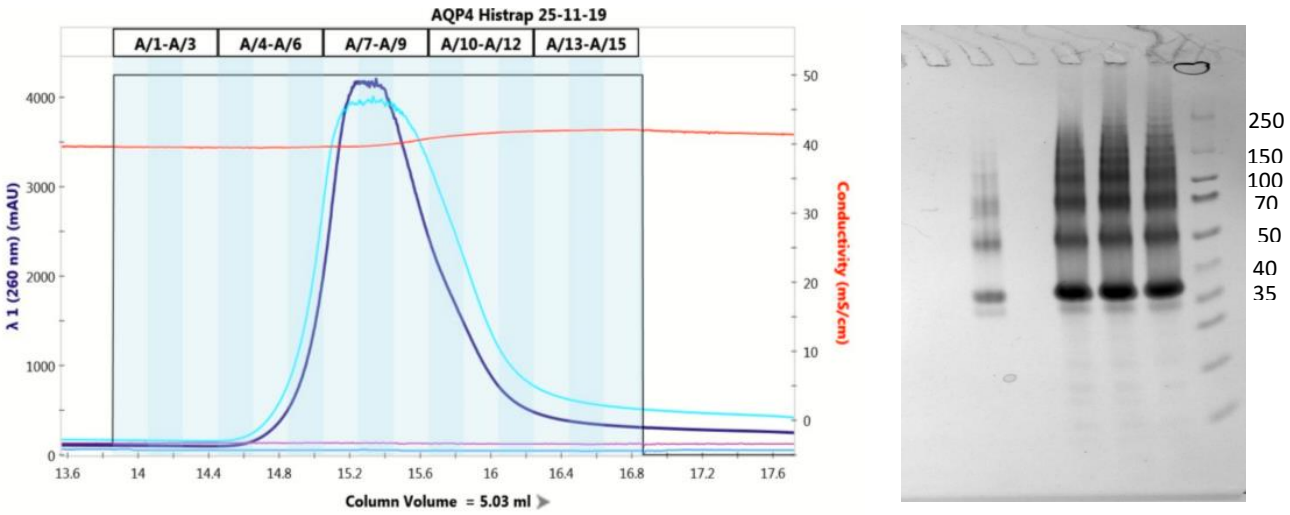

Figure4.3.1 chromatogram of affinity chromatography (His-trap), represent the AQP4 elution with high imidazole concentration. SDS-PAGE result illustrate the appearance of the monomer, dimer and tetramer structure of AQP4 with MWt= 36 kDa .

The chromatogram shows elution of the AQP4 in a high intense peak which means that the OG serves as beneficial detergent to extract a high amount of the protein from the membrane. The extraction of the AQP4 from cells was also possible using OGNG as detergent but it might interfere to the next analysis. The concentration of (300 mM) imidazole was enough to elute the sample from column. The SDS-PAGE illustrates the pure AQP4 with monomer dimer and tetramer structure.

Fractions containing AQP4, was concentrated to 10 mg/ml and loaded into the gel filtration column. The chromatogram (Figure 4.3.2) displayed two peaks, the first peak belongs to aggregated or unhappy protein, while the second peak was the healthy AQP4 used for nanodisc preparation.

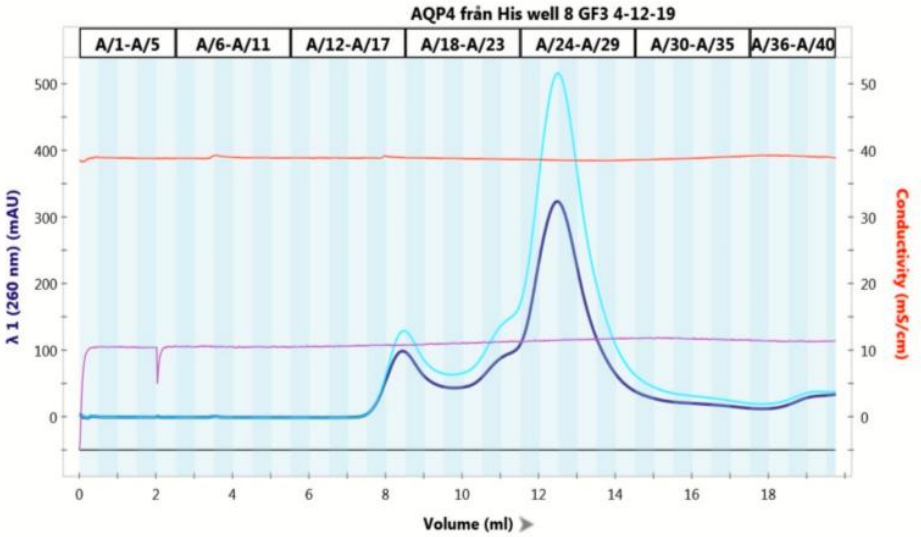

Figure4.3.2 chromatogram superdex Gel filtration, run in order to improve sample homogeneity and removing the excess of glycerol from the sample mixture.

4.4. Nanodisc purification

The nanodisc complex needed to be purified from empty nanodisc and the free AQP4 which was not incorporated into any nanodisc. First purification step was done with 1ml His-Trap column in order to separate empty nanodiscs and nanodiscs containing AQP4. Removal of His-tag in MSP was useful in this step, the nanodisc itself doesn't contain His-tag, which leads to no interaction between this nanodisc and the column, while the AQP4 still has the Histidine residue, that make the nanodisc containing AQP4 bind tightly to the column and be separated from the empty nanodisc. Using 0.3 M of imidazole leads to the elution of the nanodisc containing AQP4 from the column. The first peak in the chromatogram (Figure 4.4.1) illustrates the empty nanodiscs, while the second peak represent to nanodisc containing AQP4.

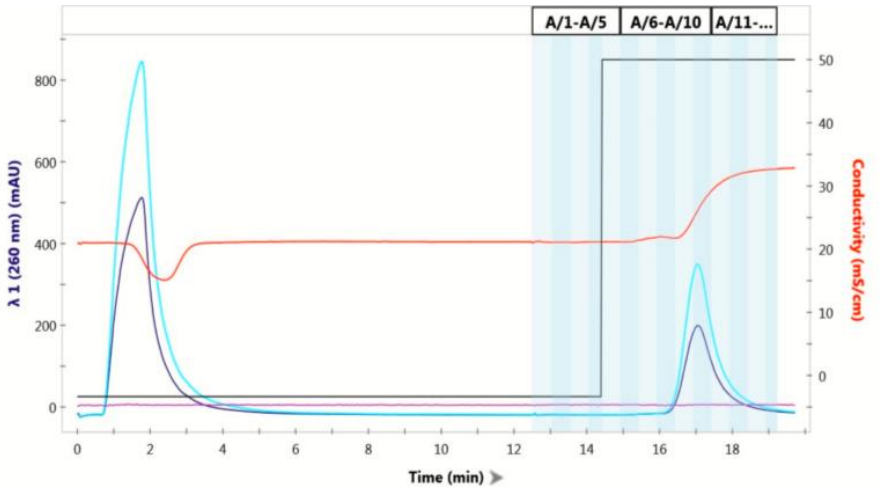

Figure 4.4.1. chromatogram result for nanodisc purification using 1 ml His-tarp column, the first peak belongs to empty nanodisc, while the second peak which had been eluted with high concentration of imidazole belong to nanodisc complex.

Further purification with gel filtration was done in order to ensure the nanodisc complex homogeneity by removing the excess of AQP4 which had not been incorporated into the nanodisc but bound to the Ni-column. The result of purification of nanodisc complex was the chromatogram below (Figure 4.4.2). The purified sample concentration was measured by nanodrop to be 1.73 mg/ml in 50 µl. This sample was quite enough to send it for Cryo-EM analysis.

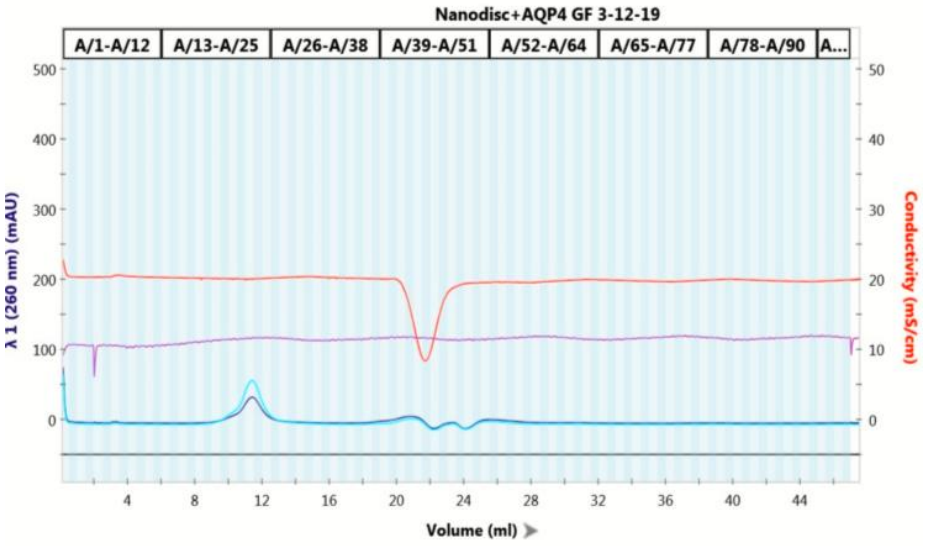

Figure 4.4.2. nanodisc purification by superdex200 gel filtration the AQP4 in nanodisc was pure enough for Cryo-EM analysis.

4.5. Cryo-EM AQP4 complex

The full length AQP4 was successfully reconstituted into the nanodiscs. The nanodiscs containing membrane protein were then treated with the activated CaM to form the complex. The complex was further analyzed using Cryo-EM. The micrograph results of Cryo-EM showed that the particles were evenly distributed in the grids holes (Figure A 4.5.1). Cryo-EM data processing was done using cryosparc following the patch-motioncorrection, patch-CTF routine. Template-free particle picking was done using 100 images and particles were extracted with a box size of 320 pixels. After 2D classification, the good 2D classes were used as template to pick in total 426K particles from the whole dataset (FigureB 4.5.1). The resolution of the final map could only reach 13 Å in the initial data analysis.

A

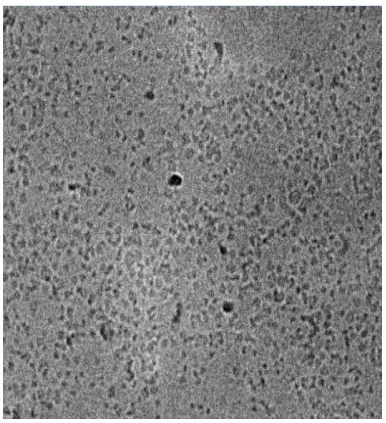

B

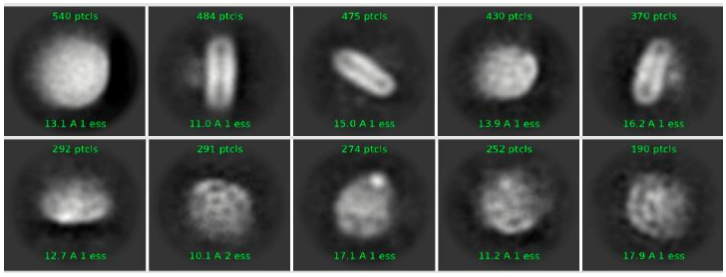

Figure 4.5.1. Cryogenic electron microscopy (Cryo-EM) data collection and analysis (A) a representative Cryo-EM micrograph collected on a Titan Krios microscope operate at 300 KV. (B) 2D class average of the almost 10 populated classes out of more than a few hundred thousand particles.

The Cryo-EM density map (Figure 4.5.2) represents the structure of nanodisc where the AQP4 is supposed to be docked on the top of the disc. The two bulges below the map could be represent the two molecule of CaM that bind to the C-terminal of AQP4, in our case, and the AQP4 is located in the side of the disc.

A

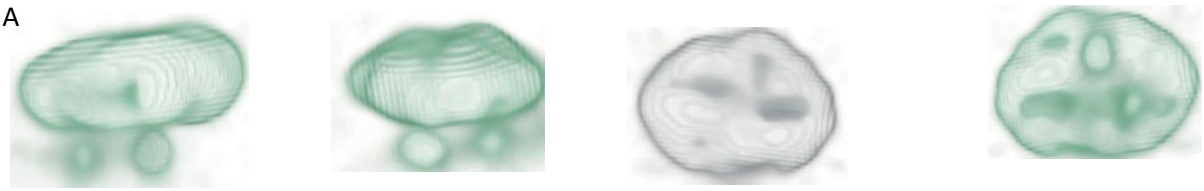

Side view Front view Top view Bottom view

B

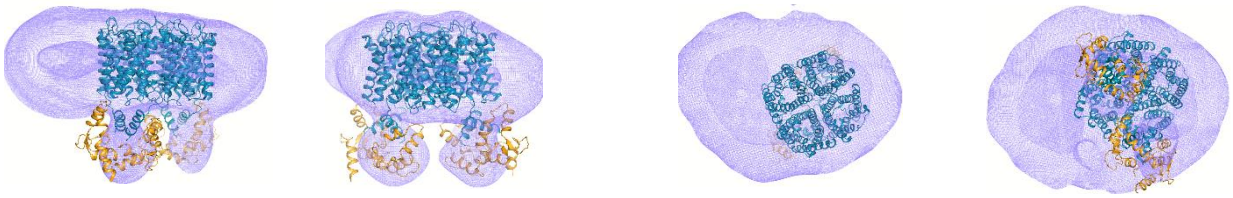

Figure 4.5.2. (A).Cryo-EM density map of the AQP4- CaM complex).(B) Figures made by Pymol represent a rigid body docking of the AQP0 -CaM complex).

As it is clear form Cryo-EM map density the size of the disk was bigger than the AQP4, which caused the protein to be located to the one side of the nanodisc. Smaller MSP belt would be beneficial in order to characterize and clarify the structure of AQP4. By changing the size of the belt, the ratio that had been used for nanodisc assembling should be altered.

25 Å cryo-EM pseudoatomic model of AQP0-CaM has been recently published. This model suggests that each CaM molecule bind to antiparallel C-terminal helices of AQP0 (Figure 4.5.2) in cooperative manner, so that each tetramer of AQP0 can bind to two CaM molecules. This binding of CaM to AQP0 lead to inhibition of water transport. The exact mechanism of how the water is inhibited by CaM remain poorly understand. As the AQP4 share the same structure properties with AQP0 we fitted the AQP0-CaM model into the cryo-EM map for the AQP4-CaM complex. As seen in Figure 4.5.2, the model fitted quite well, with the two CaM -molecules ending up in the small densities below the disc. This supports that AQP4 binds two copies of CaM in a similar manner as seen for AQP0.

5.Conclusion & further optimization

One of the most challenging technique in the structural biology is, quantification of protein-protein interaction involving the membrane proteins. The reason come from the fact that MP have low sample availability and need the detergent to be extracted. In this study we showed that the Cryo-EM could be used in order to study the interaction between full-length AQP4 and CaM using a low amount of the sample. Further the full-length AQP4 showed to bind to CaM directly. In this study we used the nanodisc to have the AQP4 in the most stable form, by removing the detergent.

The AQP4 was successfully reconstituted into the nanodisc. There are still many parameters that could be optimized in order to increase the yields of the nanodisc containing AQP4, such as the ratio of MP:lipid:MSP, amount of bio beads added to the mixture, detergent, type of phospholipid, size of MSP and incubation time for nanodisc assembly.

The Cryo-EM structure of the complex made of AQP4 and Calmodulin, provides structural information about that the AQP4 could be regulated by protein-protein interaction. we show from Cryo-EM density that the two CaM molecule are binding directly to the AQP4 from cytosolic side.

In order to prove the protein-protein interaction, the sample could be further analyzed using MST technique. This technique allows to measure the binding constant of any type of bimolecular interaction such as protein-protein interaction, In this case AQP4-CaM.

Instead of using detergent it may be more beneficial to use Styrene malic acid (SMA) as copolymer, for the solubilization, purification and characterization of AQP4. The advantage of this method is that you can skip lots of purification method and have the protein in the form of nanodisc from the solubilization step. By this method we can have the protein in an environment quite like a natural environment. One will always lose sample during, protein solubilization, purification and incorporating in the nanodisc. By this method we can escape the nanodisc preparation and save quite large amount protein. The purified protein using SMA could be used directly for Cryo-EM.

Treating the AQP4 with the calmodulin (after nanodisc assembling) to form the complex, by that the remaining CaM could be removed during purification and the resulting complex will be pure for Cryo-EM analysis.

Appendix

Table 1: recipe to make 500 ml of LB agar plate

LB-AGAR	
NaCl	5g
Tryptone	5g
Yeast Extract	2.5
Agar	7.5
H_2O	Add to 500 ml

Table 2: recipe for 500ml LB media preparation

LB-Media	
Tryptone	5 g
Yeast Extract	2.5 g
NaCl	5 g
H_2O	Add to 500 ml

Table 3: recipe for 1 LTB media preparation

TB-Media	
Tryptone	12 g
Yeast Extract	24 g
Glycerol	4 ml
KH_2PO_4	2.31 g
K_2HPO_4	12.54 g
H_2O	Add to 1 L

Table 4: KPO_4 buffer, the buffer that we used for MSP pellet storage doesn't contain imidazole

KPO_4 buffer	
KPO_4	20mM
NaCl	0.1 M
pH= 7.4	

Table 5: washing buffer used for MSP purification before removal of his-tag.

Buffer 1 (MSP)	40ml, pH=8
Tris-HCl	40mM
NaCl	0.3 M
Triton X-100	1%

Table 6: washing buffer 2, used for MSP purification before removal of His-tag.

Buffer 2 (MSP)	40ml, pH= 8
Tris-HCl	40mM
NaCl	0.3 M
Na-cholate	50mM
Imidazole	20mM

Table 7: buffer 3, MSP purification before His-tag cleavage

Buffer 3 (MSP)	40ml,pH=8
Tris-HCl	40mM
NaCl	0,3 M
Imidazole	50 mM

Table 8: buffer 4, MSP purification

Buffer 4 (MSP)	40ml, pH= 8
Tris-HCl	40mM
NaCl	0.3 M
Imidazole	400mM

Table 9: dialysis buffer for MSP, against imidazole buffer

Tris-buffer	1 L, pH=7.5
Tris-HCl	20mM
NaCl	0.1 M

Table 10: buffer used for column equilibration after removal of His-tag from MSP

Equilibration buffer	40ml, pH=7.5
Tris-HCl	20mM
NaCl	0.1 M
Imidazole	20 mM

Table 11: recipe for YPD-media and (agar)

YPD	
Yeast	10 g
Peptone	20 g
Dextrose	20 g
(Agar)	20 g
H_2O	Add to 1L

Table 12: BSM media for P.pastoris over expression using the fermenter

BSM (1.5 L)	
Calcium sulphate	1.395 g
Potassium Sulphate	27.3 g
Magnesium Sulphate×7 H_2O	22.305 g
Potassium Hydroxide	6.195 g
Glycerol 99%	60.3 ml
Phosphoric acid 85%	40.05 ml
H_2O	Add to 1.5 L

Table 13: PTM recipe used during expression of P.pastoris.

PTM (100 ml)	
Cupric Sulphate	0.6 g
Sodium Iodide	8 mg
MagnesiumSulphate×7H2O	0.3 g
Sodium molybdate×2 H2O	0.02 g
Cobalt Chloride	0.05 g
Boric Acid	2 mg
Zink Chloride	2g
Ferrous sulphate×7H2O	6.5 g
Biotin	0.02 g
Sulphuric acid	500 µl
H2O	Add to 100ml

Table 14: Breaking buffer, used to breaks P.pastoris cells

Breaking buffer (AQP4)	500ml, pH=7.5
KPi	50 mM (25 ml)
Glycerol	5% (25 ml)
EDTA	2 mM (2ml)

Table 15: Urea buffer membrane prep protocol

Urea buffer (AQP4)	500ml, pH=9.5
Tris-HCl	50mM (25 ml)
Urea	4 M (120.12g)
EDTA	2 mM (2 ml)

Table 16: membrane buffer (membrane preparation protocol) suitable for membrane storage

Membrane buffer (AQP4)	500ml, pH=8
Tris-HCl	50mM (25 ml)
NaCl	20 mM (2 ml)
Glycerol	10% (50 ml)

Table 17: solubilization buffer, buffer containing detergent, with aim of extracting the protein from membrane.

Solubilization buffer (AQP4)	25 ml, pH=8
Tris-HCl	20mM (500µl)
NaCl	150 mM (1.5 ml)
Glycerol	10% (2.5ml)
OG (solgrade)	8% (2 g)
PMSF	1mM

Table 18: Buffer A for AQP4 purification using His-Trap

Buffer A (AQP4)	400 ml, pH=8
Tris-HCl	20mM
NaCl	300 mM
Glycerol	10%
OG (Anagrade)	1%

Table 19: buffer B, elution of AQP4 in column

Buffer A (AQP4)	400 ml, pH=8
Tris-HCl	20mM
NaCl	300 mM
Glycerol	10%
OG (Anagrade)	1%
Imidazole	300 mM

Note: running buffer for SEC column doesn't contain Glycerol.

Table 20: X ml stock for MES buffer. The running buffer that had been used was 1X .

Nu-PAGE MES buffer 10X	
MES	19.52 g
EDTA	0.6 g
Bis-Tris	12.12 g
SDS	2 g

Table 21: sodium cholate buffer, used to solubilize POPC, for nanodisc preparation.

Sodium-cholate for POPC (1ml)	
Sodium cholate	100 mM
NaCl	100 mM
Tris pH=8	20 mM
H_2O	Add to 1 ml

Table 22: Buffer A, His-trap equilibration, nanodisc.

Buffer A nanodisc purification	
Tris pH=8	20mM
NaCl	150 mM
H_2O	Add to 250 ml

Table 23: elution buffer, His-trap, nanodisc pur.

Elution buffer nanodisc purification	
Tris pH=8	20mM
NaCl	150 mM
Imidazole	300 mM
H_2O	Add to 50 ml

7.References

[1] H. Bloemendal, A. Zweers, F. Vermorken, I. Dunia, and E. L. Benedetti, 'The plasma membranes of eye lens fibres. Biochemical and structural characterization', *Cell Differ.*, vol. 1, no. 2, pp. 91–106, Jun. 1972, doi: 10.1016/0045-6039(72)90032-2.

[2] G. Benga, 'The first water channel protein (later called aquaporin 1) was first discovered in Cluj-Napoca, Romania', *Romanian J. Physiol. Physiol. Sci.*, vol. 41, no. 1–2, pp. 3–20, Jun. 2004.

[3] E. Kruse, N. Uehlein, and R. Kaldenhoff, 'The aquaporins', *Genome Biol.*, vol. 7, no. 2, p. 206, 2006, doi: 10.1186/gb-2006-7-2-206.

[4] P. Agre, 'The Aquaporin Water Channels', *Proc. Am. Thorac. Soc.*, vol. 3, no. 1, pp. 5–13, Mar. 2006, doi: 10.1513/pats.200510-109JH.

[5] Y. Wang and E. Tajkhorshid, 'Nitric Oxide Conduction by the Brain Aquaporin AQP4', *Proteins*, vol. 78, no. 3, pp. 661–670, Feb. 2010, doi: 10.1002/prot.22595.

[6] P. Agre *et al.*, 'Aquaporin water channels – from atomic structure to clinical medicine', *J. Physiol.*, vol. 542, no. Pt 1, pp. 3–16, Jul. 2002, doi: 10.1113/jphysiol.2002.020818.

[7] D. Liénard *et al.*, 'Water Transport by Aquaporins in the Extant Plant Physcomitrella patens', *Plant Physiol.*, vol. 146, no. 3, pp. 1207–1218, Mar. 2008, doi: 10.1104/pp.107.111351.

[8] X.-G. Guan *et al.*, 'NPA motifs play a key role in plasma membrane targeting of aquaporin-4', *IUBMB Life*, vol. 62, no. 3, pp. 222–226, 2010, doi: 10.1002/iub.311.

[9] E. Beitz, B. Wu, L. M. Holm, J. E. Schultz, and T. Zeuthen, 'Point mutations in the aromatic/arginine region in aquaporin 1 allow passage of urea, glycerol, ammonia, and protons', *Proc. Natl. Acad. Sci.*, vol. 103, no. 2, pp. 269–274, Jan. 2006, doi: 10.1073/pnas.0507225103.

[10] M. Hara-Chikuma and A. S. Verkman, 'Physiological roles of glycerol-transporting aquaporins: the aquaglyceroporins', *Cell. Mol. Life Sci. CMLS*, vol. 63, no. 12, pp. 1386–1392, Jun. 2006, doi: 10.1007/s00018-006-6028-4.

[11] A. S. Verkman, 'Aquaporins', *Curr. Biol. CB*, vol. 23, no. 2, pp. R52–R55, Jan. 2013, doi: 10.1016/j.cub.2012.11.025.

[12] V. Nesverova and S. Törnroth-Horsefield, 'Phosphorylation-Dependent Regulation of Mammalian Aquaporins', *Cells*, vol. 8, no. 2, p. 82, Feb. 2019, doi: 10.3390/cells8020082.

[13] S. Törnroth-Horsefield, K. Hedfalk, G. Fischer, K. Lindkvist-Petersson, and R. Neutze, 'Structural insights into eukaryotic aquaporin regulation', *FEBS Lett.*, vol. 584, no. 12, pp. 2580–2588, Jun. 2010, doi: 10.1016/j.febslet.2010.04.037.

[14] C. Tournaire-Roux *et al.*, 'Cytosolic pH regulates root water transport during anoxic stress through gating of aquaporins', *Nature*, vol. 425, no. 6956, pp. 393–397, Sep. 2003, doi: 10.1038/nature01853.

[15] A. Frick, M. Järvå, and S. Törnroth-Horsefield, 'Structural basis for pH gating of plant aquaporins', *FEBS Lett.*, vol. 587, no. 7, pp. 989–993, 2013, doi: 10.1016/j.febslet.2013.02.038.

[16] S. Törnroth-Horsefield *et al.*, 'Structural mechanism of plant aquaporin gating', *Nature*, vol. 439, no. 7077, pp. 688–694, Feb. 2006, doi: 10.1038/nature04316.

[17] A. S. Verkman, J. Ruiz-Ederra, and M. H. Levin, 'FUNCTIONS OF AQUAPORINS IN THE EYE', *Prog. Retin. Eye Res.*, vol. 27, no. 4, pp. 420–433, Jul. 2008, doi: 10.1016/j.preteyeres.2008.04.001.

[18] T. Katsura *et al.*, 'Constitutive and regulated membrane expression of aquaporin 1 and aquaporin 2 water channels in stably transfected LLC-PK1 epithelial cells.', *Proc. Natl. Acad. Sci.*, vol. 92, no. 16, pp. 7212–7216, Aug. 1995, doi: 10.1073/pnas.92.16.7212.

[19] A. C. Conner, R. M. Bill, and M. T. Conner, 'An emerging consensus on aquaporin translocation as a regulatory mechanism', *Mol. Membr. Biol.*, vol. 30, no. 1, pp. 101–112, Feb. 2013, doi: 10.3109/09687688.2012.743194.

[20] H. Chu *et al.*, 'Aquaporin-4 and Cerebrovascular Diseases', *Int. J. Mol. Sci.*, vol. 17, p. 1249, Aug. 2016, doi: 10.3390/ijms17081249.

[21] M. T. Conner, A. C. Conner, J. E. P. Brown, and R. M. Bill, 'Membrane Trafficking of Aquaporin 1 Is Mediated by Protein Kinase C via Microtubules and Regulated by Tonicity', *Biochemistry*, vol. 49, no. 5, pp. 821–823, Feb. 2010, doi: 10.1021/bi902068b.
[22] M. C. Papadopoulos and A. S. Verkman, 'Aquaporin 4 and neuromyelitis optica', *Lancet Neurol.*, vol. 11, no. 6, pp. 535–544, Jun. 2012, doi: 10.1016/S1474-4422(12)70133-3.
[23] I. Pirici *et al.*, 'Inhibition of Aquaporin-4 Improves the Outcome of Ischaemic Stroke and Modulates Brain Paravascular Drainage Pathways', *Int. J. Mol. Sci.*, vol. 19, no. 1, Dec. 2017, doi: 10.3390/ijms19010046.
[24] A. Rossi, T. J. Moritz, J. Ratelade, and A. S. Verkman, 'Super-resolution imaging of aquaporin-4 orthogonal arrays of particles in cell membranes', *J. Cell Sci.*, vol. 125, no. 18, pp. 4405–4412, Sep. 2012, doi: 10.1242/jcs.109603.
[25] H. Saini, G. Fernandez, D. Kerr, and M. Levy, 'Differential expression of aquaporin-4 isoforms localizes with neuromyelitis optica disease activity', *J. Neuroimmunol.*, vol. 221, no. 1–2, pp. 68–72, Apr. 2010, doi: 10.1016/j.jneuroim.2010.02.007.
[26] J. V. Roche and S. Törnroth-Horsefield, 'Aquaporin Protein-Protein Interactions', *Int. J. Mol. Sci.*, vol. 18, no. 11, Oct. 2017, doi: 10.3390/ijms18112255.
[27] Y. Yukutake and M. Yasui, 'Regulation of water permeability through aquaporin-4', *Neuroscience*, vol. 168, no. 4, pp. 885–891, Jul. 2010, doi: 10.1016/j.neuroscience.2009.10.029.
[28] B. V *et al.*, 'An aquaporin-4/transient receptor potential vanilloid 4 (AQP4/TRPV4) complex is essential for cell-volume control in astrocytes.', *Proc. Natl. Acad. Sci. U. S. A.*, vol. 108, no. 6, 00:00:00.0, doi: 10.1073/pnas.1012867108.
[29] F. Guilak, H. A. Leddy, and W. Liedtke, 'Transient receptor potential vanilloid 4: The sixth sense of the musculoskeletal system?', *Ann. N. Y. Acad. Sci.*, vol. 1192, pp. 404–409, Mar. 2010, doi: 10.1111/j.1749-6632.2010.05389.x.
[30] Alessandro Alaimo and Alvaro Villarroel, 'Calmodulin: A Multitasking Protein in Kv7.2 Potassium Channel Functions', *Biomolecules*, no. 3, p. 57, 2018, doi: 10.3390/biom8030057.
[31] S. Luan, J. Kudla, M. Rodriguez-Concepcion, S. Yalovsky, and W. Gruissem, 'Calmodulins and Calcineurin B–like Proteins', *Plant Cell*, vol. 14, no. Suppl, pp. s389–s400, 2002, doi: 10.1105/tpc.001115.
[32] M. T. Swulius and M. N. Waxham, 'Ca2+/Calmodulin-dependent Protein Kinases', *Cell. Mol. Life Sci. CMLS*, vol. 65, no. 17, pp. 2637–2657, Sep. 2008, doi: 10.1007/s00018-008-8086-2.
[33] A. P. Ferretti, R. Bhargava, S. Dahan, M. G. Tsokos, and G. C. Tsokos, 'Calcium/Calmodulin Kinase IV Controls the Function of Both T Cells and Kidney Resident Cells', *Front. Immunol.*, vol. 9, 2018, doi: 10.3389/fimmu.2018.02113.
[34] M. Zhang *et al.*, 'Structural basis for calmodulin as a dynamic calcium sensor', *Struct. England1993*, vol. 20, no. 5, pp. 911–923, May 2012, doi: 10.1016/j.str.2012.03.019.
[35] N. V. Kovalevskaya *et al.*, 'Structural analysis of calmodulin binding to ion channels demonstrates the role of its plasticity in regulation', *Pflüg. Arch. - Eur. J. Physiol.*, vol. 465, no. 11, pp. 1507–1519, Nov. 2013, doi: 10.1007/s00424-013-1278-0.
[36] T. H. Bayburt and S. G. Sligar, 'Self-assembly of single integral membrane proteins into soluble nanoscale phospholipid bilayers', *Protein Sci. Publ. Protein Soc.*, vol. 12, no. 11, pp. 2476–2481, Nov. 2003.
[37] T. H. Bayburt and S. G. Sligar, 'Membrane protein assembly into Nanodiscs', *FEBS Lett.*, vol. 584, no. 9, pp. 1721–1727, 2010, doi: 10.1016/j.febslet.2009.10.024.
[38] T. H. Bayburt, Y. V. Grinkova, and S. G. Sligar, 'Assembly of single bacteriorhodopsin trimers in bilayer nanodiscs', *Arch. Biochem. Biophys.*, vol. 450, no. 2, pp. 215–222, Jun. 2006, doi: 10.1016/j.abb.2006.03.013.
[39] T. H. Bayburt, Y. V. Grinkova, and S. G. Sligar, 'Self-Assembly of Discoidal Phospholipid Bilayer Nanoparticles with Membrane Scaffold Proteins', *Nano Lett.*, vol. 2, no. 8, pp. 853–856, Aug. 2002, doi: 10.1021/nl025623k.
[40] 'Reconstitution of Membrane Proteins in Phospholipi...: Full Text Finder'. http://resolver.ebscohost.com.ludwig.lub.lu.se/openurl?sid=EBSCO:edselp&genre=chapter&issn

=00766879&isbn=9780123749697&volume=464&issue=&date=20090101&spage=211&pages=211-231&title=Methods%20in%20Enzymology&atitle=Chapter%20Eleven%20-%20Reconstitution%20of%20Membrane%20Proteins%20in%20Phospholipid%20Bilayer%20Nanodiscs&btitle=Methods%20in%20Enzymology&jtitle=Methods%20in%20Enzymology&series=&aulast=Ritchie%2C%20T.K.&id=DOI:10.1016/S0076-6879(09)64011-8 (accessed Mar. 22, 2020).

[41] 'Single-Particle Cryo-Electron Microscopy: Mathemat...: Full Text Finder'. http://resolver.ebscohost.com.ludwig.lub.lu.se/openurl?sid=EBSCO:edseee&genre=article&issn=10535888&isbn=&volume=37&issue=2&date=20200301&spage=58&pages=58-76&title=IEEE%20Signal%20Processing%20Magazine,%20Signal%20Processing%20Magazine,%20IEEE,%20IEEE%20Signal%20Process.%20Mag.&atitle=Single-Particle%20Cryo-Electron%20Microscopy:%20Mathematical%20Theory,%20Computational%20Challenges,%20and%20Opportunities&btitle=IEEE%20Signal%20Processing%20Magazine,%20Signal%20Processing%20Magazine,%20IEEE,%20IEEE%20Signal%20Process.%20Mag.&jtitle=IEEE%20Signal%20Processing%20Magazine,%20Signal%20Processing%20Magazine,%20IEEE,%20IEEE%20Signal%20Process.%20Mag.&series=&aulast=Bendory,%20T.&id=DOI:10.1109/MSP.2019.2957822 (accessed Apr. 14, 2020).

[42] M. Liao, E. Cao, D. Julius, and Y. Cheng, 'Structure of the TRPV1 ion channel determined by electron cryo-microscopy', *Nature*, vol. 504, no. 7478, pp. 107–112, Dec. 2013, doi: 10.1038/nature12822.